

Morphological, structural and optical properties of Al-doped ZnO nanosheet arrays influenced by pulsed electromagnetic field

Jianzhong Wang¹, Li-dan Tang¹, Bing Wang¹, Huiling Du², Jingang Qi¹, Shujing Peng²

¹School of Materials Science and Engineering, Liaoning University of Technology, Jinzhou 121001, People's Republic of China

²School of Chemical and Environmental Engineering, Liaoning University of Technology, Jinzhou 121001,

People's Republic of China

E-mail: kittytld@yahoo.com.cn

Published in Micro & Nano Letters; Received on 11th November 2012; Revised on 22nd January 2013; Accepted on 1st February 2013

High-quality Al-doped ZnO nanosheet arrays have been prepared by hydrothermal methods assisted with the pulsed electromagnetic field (PEMF). These effects of PEMF on the morphology and structural properties of Al-doped ZnO nanosheet arrays were studied in detail. Results showed Al-doped ZnO nanosheet arrays with PEMF had better orientation, more density, a greater ratio of diameter to thickness and stronger ultraviolet emission peak than those without PEMF. Finally, a possible mechanism of PEMF acting on Al-doped ZnO nanosheet arrays is proposed.

1. Introduction: Dye-sensitised solar cells (DSSCs) have shown their competence as one of the potential candidates for the next generation of solar cells because of their high efficiency, low cost, environmental friendliness, low-angle dependency on incident light and many other advantages [1, 2]. So far, many kinds of DSSCs have been developed [3–7]. Among them, dye-sensitised solar cells based on one-dimensional (1D) ZnO nanostructures have attracted a lot of scientific and technological interest in recent years. However, the cell efficiency based on the 1D ZnO nanostructure is still low because of large inherent resistances [8]. Al-doped ZnO nanostructure films show comparable electrical and optical properties [9]. Hence, it is estimated that Al-doped ZnO nanostructure films as an anode can maximise cell efficiency. However, the key point for the DSSCs is to produce a well-ordered Al-doped ZnO nanostructure. Hydrothermal methods are suitable and economical in obtaining 1D ZnO nanostructures [10–13]. Also, the ultraviolet-irradiation method and extra field technology has been introduced to obtain uniform and high-quality nanomaterials. The results indicated that the extra field plays a key role in crystal growth [14]. In this Letter, we discuss the effects of the pulsed electromagnetic field (PEMF) on the morphological, structural and optical properties of Al-doped ZnO nanostructure films. Furthermore, a possible mechanism of PEMF acting on crystal growth is discussed.

2. Experimental: Al-doped ZnO nanosheet arrays were prepared on the fluorine doped tin oxide (FTO) substrates by hydrothermal methods assisted with PEMF. FTO substrate is a kind of electric glass with the content of F-doped SnO₂ films. FTO substrates were coated with ZnO seeds. ZnC₄H₁₀O₆ (zinc acetate dihydrate), CH₃COONH₄ (IUPAC: (3R)-3-[4-(2-chlorophenyl)piperazin-1-yl]-1-(3-methoxyphenyl)) and HOCH₂CH₂OCH₃ (IUPAC: 2-methoxyethanol) were mixed to form a solution where the volume ratios are 1:1.5:7.5. The solution was deposited on FTO substrate by a spin coater (TB-616, China) and then heated at 300°C for 10 min to form ZnO seeds films. Zn(NO₃)₂, Al(NO₃)₃ and C₆H₁₂N₄ (2-butyl-1-cyanoguanidine) were mixed in deionised water to form a reactive aqueous solution. The molar ratios of Zn(NO₃)₂, Al(NO₃)₃ and C₆H₁₂N₄ are 0.97:0.03:1. All the reagents used in our experiments were analytical grade and employed without any further purification and treatment. Then reactive aqueous solutions were put slowly into the teflon lined autoclave and pre-coated FTO substrates were immersed in the solution. PEMF was applied to the solution for 1 min, as shown in Fig. 1. The PEMF equipment is patented [15]. The voltage and

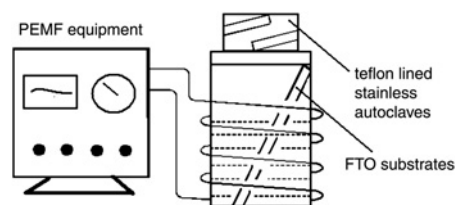


Figure 1 Sketch map of PEMF applied to solution

frequency of the PEMF is 500 V and 4 Hz, respectively, and the electromagnetic intensity on the axis of the solenoidal inductor ranged from 1.42 to 2.31 T. A hydrothermal reaction was carried out at the appointed temperature of 95°C for 4 h. Thus, sample A was obtained. On the other hand, sample B was prepared under similar conditions as those of sample A, but without the presence of PEMF. After the reaction, the teflon lined autoclave was cooled naturally to room temperature, and the substrates with as-grown Al-doped ZnO nanosheet arrays were rinsed repeatedly with deionised water to remove the residual reactants.

The crystalline structure of the obtained ZnO nanorod arrays was analysed by X-ray diffraction (XRD) (D\max-2500\pc). The morphology of ZnO nanorod arrays was characterised by using field emission scanning electron microscopy (FESEM) (Zeiss, SUPRA-55). Photoluminescence (PL) spectrum was measured by a LabRam Raman spectrometer (SPEX 1403) and excited by a 325 nm He–Cd laser source.

3. Results and discussion: Fig. 2 shows SEM images of Al-doped ZnO nanosheet arrays prepared with PEMF and without PEMF. Figs. 2a and b show the plan form and the side elevation of Al-doped ZnO nanosheet films fabricated by hydrothermal methods with PEMF (sample A). These products look like flat hexagonal sheets that are interlaced with each other regularly. All Al-doped ZnO nanosheet arrays grow vertically on the FTO substrate. Figs. 2c and d are taken from the plan form and the side elevation of the ZnO nanostructure using hydrothermal methods without PEMF (sample B), respectively. Sample B looks like an almost hexagonal shape but these Al-doped ZnO nanosheet arrays are not arranged in order. Most nanosheets grow vertically on the FTO substrate but some nanosheets lie on the arrays. As a result, well-aligned Al-doped ZnO nanosheet arrays with PEMF have better verticality on the substrate and more density than those without PEMF.

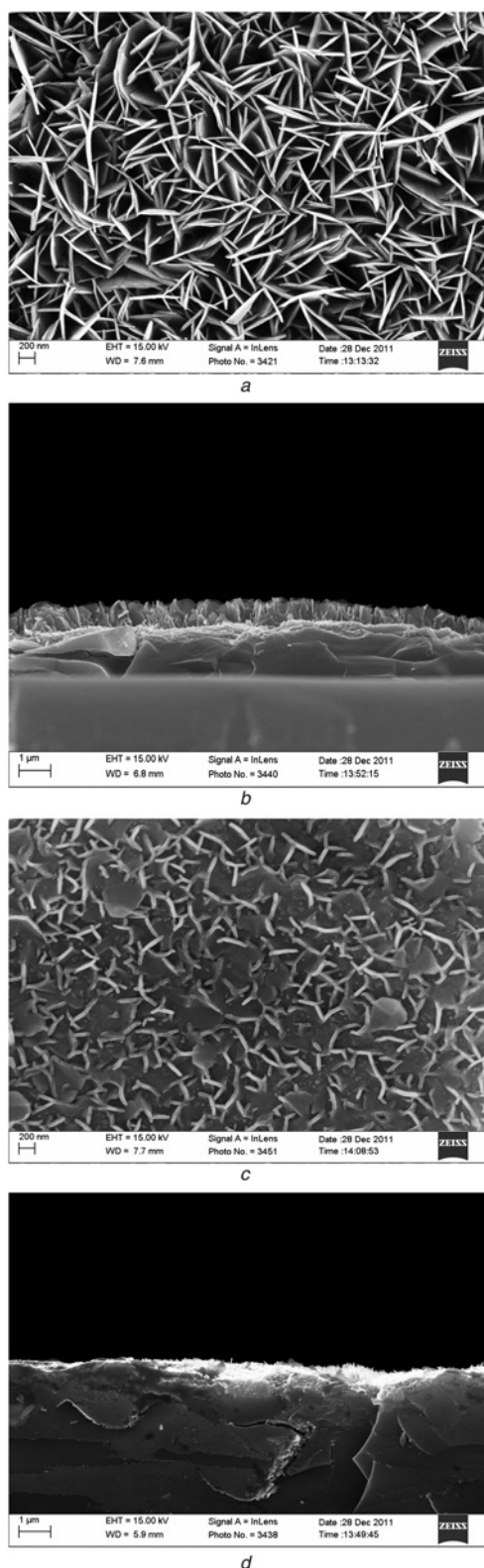


Figure 2 SEM images of Al-doped ZnO nanosheet arrays
a Plan form of sample A prepared with PEMF
b Side elevation of sample A prepared with PEMF
c Plan form of sample B prepared without PEMF
d Side elevation of sample A prepared without PEMF

Fig. 3 shows the EDS results of Al-doped ZnO nanosheet arrays. According to the EDS analysis the Al element content of Al-doped ZnO nanosheet arrays with PEMF and without PEMF is 1.78 at% (± 0.25 at% error) and 1.54 at% (± 0.23 at% error). The actual Al element content in ZnO is lower than the theoretical content

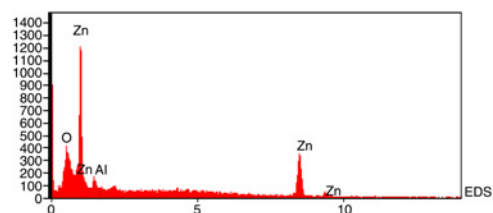


Figure 3 EDS pattern of Al-doped ZnO nanosheets prepared with PEMF

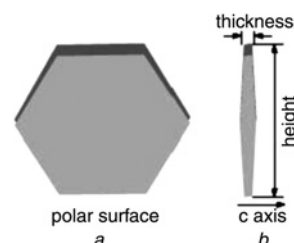


Figure 4 Schematic illustration of ZnO nanosheet model
a Elevation
b Side elevation

because some part of the Al element had not been incorporated in ZnO in hydrothermal reaction.

According to our experimental results the proposed structural model of Al-doped ZnO nanosheet arrays is shown in Fig. 4. Al-doped ZnO nanosheet arrays are hexagonal sheets and the growth direction is vertical in comparison with the *c*-axis. It is well known that most pure ZnO should be hexagonal stubs by using hydrothermal methods [16]. However, ZnO is a hexagonal sheet as a result of the doping Al element. It is the main reason why the Al atom restricted the growth rate of the polar surface by adsorbing, so the growth rate of the unpolar surface is faster than that of the polar surface [17]. To investigate further the morphology of synthesised Al-doped ZnO nanosheet arrays, the thickness and height of the nanosheet can be observed in Fig. 2. The results are listed in Table 1. The thickness and heights of sample A prepared with PEMF are about 18 and 780 nm, respectively. The ratio of height to thickness is 43.3 by calculation. However, the ratio of diameter to thickness of sample B prepared without PEMF is only 12.7. As a result sample A prepared with PEMF has a greater ratio of heights to thickness that rose about four times as much as that of sample B. The ZnO anode with a big ratio of height to thickness can adsorb more dye to increase the efficiency of the dye-sensitised solar energy conversion.

Fig. 5 shows XRD patterns of Al-doped ZnO nanosheet arrays using hydrothermal methods with PEMF and without PEMF. All the peaks can be indexed in the figure. Except for peaks of the Si substrate, all the other diffraction peaks could be well indexed to the standard diffraction pattern of the hexagonal phase ZnO (JCPDS36-1451). It shows that both Al-doped ZnO nanosheet arrays have a wurtzite structure with high crystallinity. According to the XRD pattern the relative intensity of diffraction peaks in both samples are different and calculated as shown in Table 2. These main diffraction faces are include (002), (103), (112) and (004), respectively. Especially, the diffraction faces (002)

Table 1 Characterisation of Al-doped ZnO nanosheet arrays with and without PEMF

Sample	Thickness, nm	Height, nm	Height/thickness
A	18	780	43.3
B	32	405	12.7

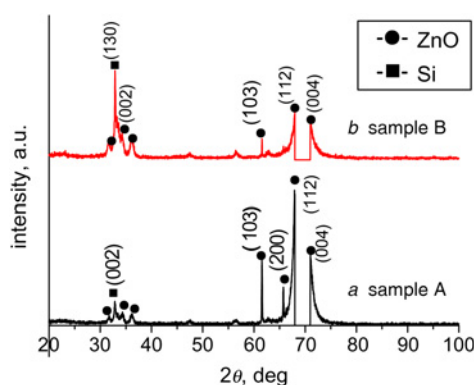


Figure 5 XRD patterns of ZnO nanosheet arrays prepared with and without PEMF
a With PEMF
b Without PEMF

Table 2 Diffraction peak intensity ratios of Al-doped ZnO nanosheets array with and without PEMF

Sample	(103)/(002)	(112)/(002)	(004)/(002)
A	5.4	11.2	6.1
B	0.7	1.7	1.5

correspond to the diffraction direction $[00\bar{1}1]$ that is along the c -axis of ZnO [18, 19]. It can be found that the intensity ratios of (103) to (002), (112) to (002) and (004) to (002) in sample A are far higher than those in sample B. The whole relative intensities of (002) diffraction peaks in sample A are lower than those in sample B, which indicates that Al-doped ZnO nanosheet arrays are not growing along the c -axis.

To investigate further the optical properties of synthesised Al-doped ZnO nanosheet arrays at room temperature, PL studies were carried out at an exciton wavelength of 325 nm and the corresponding spectrum is shown in Fig. 6. There are two main emission peaks in both Al-doped ZnO nanosheet arrays. One strong peak at ~ 375 nm was assigned to UV emission. The UV emission should be attributed to the near band-edge emission of the wide bandgap of ZnO because of the free-exciton recombination [20, 21]. The other broad peak at ~ 527 nm is green band emission. It has been suggested that the green band emission results from the surface defect levels associated with oxygen vacancies [22]. It is observed that the visible green emission of both samples is greatly enhanced and the UV emission is weakened. This result may be because of more defects originating from Al element doping.

From Fig. 6 it can be seen that both the UV and green emissions of Al-doped ZnO nanosheet arrays with PEMF (sample A) are stronger than those of Al-doped ZnO nanosheet arrays without

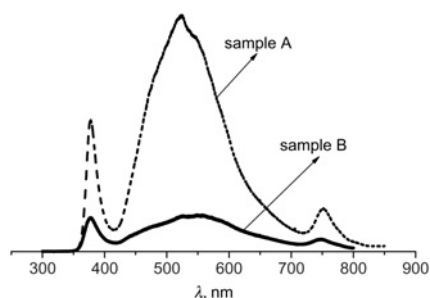


Figure 6 PL spectrum of ZnO nanosheets array prepared with and without PEMF

PEMF (sample B). This can be explained in that Al-doped ZnO nanosheet arrays with PEMF have thickness increase and high density. By increasing the thickness and density of the films, PL emission can be enhanced because of emission source quantity rising. In addition, PL emission can be easily enhanced, originating from the small tips, not from the plane [23]. However Al-doped ZnO nanosheet arrays without PEMF are not vertical and some nanosheets lie on the array, which weakened the PL emission. These results substantiate that ZnO nanosheet, arrays with PEMF have better optical properties.

According to our experimental results, PEMF plays an important role in the growth of Al-doped ZnO nanosheet arrays. Al-doped ZnO nanosheet arrays with PEMF have better verticality on the substrate and a greater ratio of heights to thickness. The possible mechanism of PEMF acting on Al-doped ZnO nanosheet arrays is discussed as follows: in a reaction solution the electriferous particles will accelerate motion under the magnetic field. The ZnO growth unit aggregated quickly to promote the growth rate of Al-doped ZnO nanosheet arrays, resulting in bigger heights and the ratio of heights to thickness. Also, anti-magnetic water molecules keep away from the polar ion because of magnetic field repellency. The nanosheets are more uniform on the substrate, resulting in better verticality and regular arrays.

4. Conclusion: In this Letter we have presented the growth and characterisation of high-quality Al-doped ZnO nanosheet arrays on FTO substrates with hydrothermal methods assisted by PEMF. The results showed that Al-doped ZnO nanosheet arrays had better verticality on the substrate, more density, a greater ratio of heights to thickness and stronger PL emission after PEMF was introduced, which is the benefit of increasing the efficiency of dye-sensitised solar energy conversion.

5. Acknowledgments: This work was supported by the Research Foundation of Education Bureau of Liaoning Province, China (grant no. L2011098), the Foundation for the Key Programme of the Ministry of Education, China (no. 212031) and the National Natural Science Foundation of China (grant no. 51074087).

6 References

- [1] Grätzel M.: 'The advent of mesoscopic injection solar cells prog', *Photovolt., Res. Appl.*, 2006, **14**, (5), pp. 429–442
- [2] Grätzel M.: 'Photoelectrochemical cells', *Nature*, 2001, **414**, (15), pp. 338–342
- [3] Grätzel M.: 'Conversion of sunlight to electric power by nanocrystalline dye-sensitized solar cells', *J. Photochem. Photobiol. A, Chem.*, 2004, **164**, (3), pp. 3–14
- [4] Aruna S.T., Tirosh S., Zaban A.: 'Nanosize rutile titania particle synthesis via a hydrothermal method without mineralizers', *J. Mater. Chem.*, 2000, **10**, (10), pp. 2388–2391
- [5] Qin Z., Huang Y., Liao Q.L.: 'Stability improvement of the ZnO nanowire array electrode modified with Al_2O_3 and SiO_2 for dye-sensitized solar cells', *Mater. Lett.*, 2012, **70**, pp. 177–180
- [6] Qin Z., Huang Y., Qi J.: 'Surface destruction and performance reduction of the ZnO nanowire arrays electrode in dye sensitization process', *Mater. Lett.*, 2011, **65**, (23–24), pp. 3506–3508
- [7] Tan W., Yin X., Zhou X.: 'Electrophoretic deposition of nanocrystalline TiO_2 films on Ti substrates for use in flexible dye-sensitized solar cells', *Electrochim. Acta*, 2009, **54**, (19), pp. 4467–4472
- [8] Longo C.D., Freitas J.L., Paoli M.D.: 'Performance and stability of TiO_2 /dye solar cells assembled with flexible electrodes and a polymer electrolyte', *J. Photochem. Photobiol. A, Chem.*, 2003, **159**, (1), pp. 33–39
- [9] Alim K.A., Fonoberov V.A., Shamsa M.: 'Micro-Raman investigation of optical phonons in ZnO nanocrystals', *J. Appl. Phys.*, 2005, **97**, (12), pp. 124313-1–124313-3
- [10] Greene L., Law M., Tan D.H.: 'General route to vertical ZnO nanowire arrays using textured ZnO seeds', *Nano Lett.*, 2005, **5**, (7), pp. 1231–1236
- [11] Vayssieres L.: 'Growth of arrayed nanorods and nanowires of ZnO from aqueous solutions', *Adv. Mater.*, 2003, **15**, (5), pp. 464–466

- [12] Greene L.E., Law M., Goldberger J.: 'Low-temperature wafer-scale production of ZnO nanowire arrays', *Chem. Int. Ed.*, 2003, **42**, (26), pp. 3031–3034
- [13] Sepulveda-Guzmana S., Reeja-Jayanc B., Revue de la E.: 'Synthesis of assembled ZnO structures by precipitation method in aqueous media', *Mater. Chem. Phys.*, 2009, **115**, (1), pp. 172–178
- [14] Du H.L., Wang J.Z., Wang B.: 'Preparation of cobalt oxalate powders with the presence of a pulsed electromagnetic field', *Powder Technol.*, 2010, **199**, (2), pp. 149–153
- [15] Wang J.Z., Cang D.Q.: CHN patent, CN98100543.8, 1998
- [16] Qin Z., Liao Q.L., Huang Y.H.: 'Effect of hydrothermal reaction temperature on growth, photoluminescence and photoelectrochemical properties of ZnO nanorod arrays', *Mater. Chem. Phys.*, 2010, **123**, (2–3), pp. 811–815
- [17] Fonoberov V.A., Alim K.A., Balandin A.A.: 'Photoluminescence investigation of the carrier recombination processes in ZnO quantum dots and nanocrystals', *Phys. Rev. B*, 2006, **73**, (16), pp. 165317-1–165317-9
- [18] Li H.J., Shi E.W., Zhong W.Z.: 'Theoretical model of anionic coordination polyhedron growth units and crystal morphology', *J. Synth. Cryst.*, 1999, **28**, (2), pp. 117–125
- [19] Cheng J.P., Zhang X.B., Luo Z.Q.: 'Oriented growth of ZnO nanostructures on Si and Al substrates', *Surf. Coat. Technol.*, 2008, **202**, (19), pp. 4681–4686
- [20] Look D.C., Reynolds C., Litton C.W.: 'Characterization of homoepitaxial p-type ZnO grown by molecular beam epitaxy', *Appl. Phys. Lett.*, 2002, **81**, (10), pp. 1830–1832
- [21] Vanheusden K., Warren W.L., Seager C.H.: 'Mechanisms behind green photoluminescence in assemblies of nano-ZnO particles/silica aerogels', *J. Appl. Phys.*, 1996, **79**, (10), pp. 7983–7990
- [22] Li F., Jiang Y., Hu L.: 'Luminescence properties of a Tb³⁺ activated long after glow phosphor', *J. Alloys Compd.*, 2009, **474**, (1–2), p. 531
- [23] Alim K.A., Fonoberov V.A., Balandin A.A.: 'Origin of the optical phonon frequency shifts in ZnO quantum dots', *Appl. Phys. Lett.*, 2005, **86**, (5), pp. 053103-1–053103-3